Deep Eutectic Solvent-Magnetite Hybrid Composite for Effective Removal of Zinc (II) Ions from Industrial Wastewater

*USMAN, A; OSUEGBA, SO; MAMMAN, S

Department of Chemistry, Nasarawa State University, Keffi, Nasarawa State, Nigeria

*Corresponding Author Email: adamuusmandoma2022@gmail.com
*ORCID: https://orcid.org/0009-0005-9495-1230
*Tel: +2348133000668

Co-Authors Email: osuegbasolomon@nsuk.edu.ng, mammansuwaibatu@nsuk.edu.ng

ABSTRACT: Zinc is one of the important trace element, but its high amount in aquatic bodies is detrimental to health. Hence, the objective of this paper was to synthesize deep eutectic solvent (DES) nanoparticles and evaluate their adsorption behavior for the removal of zinc (II) ions from industrial wastewater using appropriate standard techniques. The pseudo-first-order and pseudo-second-order models were utilised to investigate the adsorption kinetics, and the Freundlich and Langmuir isotherms were employed to assess the adsorption isotherms. The results of the kinetic study shows that the adsorption process follows the Langmuir isotherm model (0.9740) and pseudo-second-order kinetics (0.9186). At pH 7 and room temperature, the highest adsorption capacity was determined to be 22.883 mg/g. These findings indicate that DES nanoparticles may be a promising, highly effective, and ecologically benign adsorbent for extracting zinc (II) ions from wastewater.

Water pollution is a worldwide issue that has a detrimental effect on the quality of water resources and endangers human health and ecological health (Sawyer *et al.,* 2018). While zinc is an essential trace element necessary for numerous physiological activities, high amounts in aquatic habitats can affect the environment and human health (Deroche *et al.,* 2019). The World Health Organization (WHO, 2022) states that maximum zinc concentrations in drinking water are permitted to be between 3 and 5 mg/L. Zinc has been extracted using a variety of techniques, including membrane filtration (ultrafiltration, reverse osmosis, nanofiltration, electrodialysis) (Ahemd and Ahmaruzzaman*,* 2016; Singh, *et al.,* 2022), chemical precipitation (Walvekar, *et al.,* 2021), ion exchange (Bose *et al,* 2018) and electrochemical method (Larakeb *et al.,* 2016). However, these methods are often costly, energy-intensive, and may produce secondary pollutants (Larakeb *et al*., 2016). Therefore, there is a rising need for efficient, cost-effective, and environmentally friendly technologies for zinc removal from water. Heavy metal ion removal from aqueous solutions by adsorption has become a well-established and extensively researched technique (Artioli, 2017). Recent breakthroughs in materials science have introduced Deep Eutectic solvent (DES), a unique class of materials for heavy metal adsorption (Ümit *et al.,* 2024). DES are mixtures formed by

*Corresponding Author Email: adamuusmandoma2022@gmail.com
*ORCID: https://orcid.org/0009-0005-9495-1230
*Tel: +2348133000668

hydrogen bond acceptors and hydrogen bond donors that have a melting point that is lower than their components, offering advantages due to their environmentally friendly nature, low toxicity, and versatile applications (Gopal *et al.* 2019).

Hence, the objective of this paper was to synthesize deep eutectic solvent (DES) nanoparticles and evaluate their adsorption behavior for the removal of zinc (II) ions from industrial wastewater using appropriate standard techniques.

MATERIALS AND METHOD

Chemical and reagents: Choline chloride and ethylene glycol were purchased from Hopekin and Williams Limited. Otto Chemie Pvt. Ltd in Lafia, Nasarawa state, Nigeria, provided the ammonia solution, iron (III) chloride hexahydrate ($FeCl_3 \cdot 6H_2O$), iron (II) chloride tetrahydrate ($FeCl_2 \cdot 4H_2O$), and zinc sulfate heptahydrate ($ZnSO_4 \cdot 7H_2O$). All compounds were of analytical quality and utilised without further purification.

Instruments: German-made Analytik Jena AG's novAA 400 hydride generation-atomic absorption spectrophotometer (AAS). HY-5A Cycling vibrator, digital weighing balance, fume cupboard, oven, weighing balance (beam balance), and magnetic stirrer were all utilized.

Synthesis of DES Nanoparticles: This study used, with few changes, the methodology outlined by Gopal *et al.* (2019). Choline chloride and ethylene glycol were mixed in a 1:2 molar ratio to create DES. At a moderate temperature of 80 $^{\circ}$C, the mixture was gently swirled with a magnetic stirrer until a homogenous liquid was created. The DES was allowed to cool and solidify at room temperature. Fe_3O_4 nanoparticles were created by a traditional co-precipitation process utilising 5.2g $FeCl_3.6H_2O$ and 2.0g $FeCl.H_2O$ dissolved in 160 ml of deionised water, degassed with nitrogen, and agitated vigorously at 90 $^{\circ}$C. A 12 ml of ammonia solution was added and stirred for 1 hour. For future usage, the nanoparticles were cleansed with deionised water, crushed, and sieved. They were then oven-dried for a whole day. The DES was subsequently integrated into the Fe_3O_4 nanoparticles to generate DES nanoparticles.

Preparation of Zinc (II) Stock Solution: By dissolving 100 mg of $ZnSO_4 \cdot 7H_2O$ in a graduated measuring cylinder and adding deionized water to make the volume 1000 mL, a 100 mg/L zinc(II) stock solution was prepared. Using serial dilution, standard solutions with concentrations of 20, 40, 60, 80, and 100 mg/L were made from the stock solution.

Adsorption Experiments: The methods described by Stylianos *et al.* (2020) were adopted with slight modifications. The adsorption of zinc (II) ions was investigated in batch adsorption tests by varying the adsorbent dose (0.1-0.5 g/L), temperature (25-45°C), pH (3-9), contact duration (0-120 min), and initial zinc concentration (20-100 mg/L). DES nanoparticles at a specified concentration and 100 mL of zinc solution were added to 250 ml Erlenmeyer flasks for the adsorption processes. After the test solution was heated in a thermostatic water bath to the desired temperature, the adsorbent was separated using a phase separation membrane, and Zn (II) ion concentrations were determined using an AAS. The pH was adjusted by adding 0.1 M aqueous HCl or 0.1 M aqueous NaOH to the test solution, and the flask was shaken in an electro-thermostatic water bath oscillator at 170 rpm.

Data Analysis: Adsorption efficiency (R): Equation (1) was utilised to get the adsorption efficiency.

$$\%R = \frac{c_0 - c_e}{c_0} \times 100 \qquad 1$$

Where zinc (II) concentration at adsorption equilibrium (c_e) is measured in mg/L, and zinc (II) starting concentration (c_o) is expressed in mg/L.

Adsorption capacity (q_t): The adsorption capacity q_t was calculated using equation (2) and is defined as the amount of Zn (II) adsorbed per gramme (mg/g):

$$q_t = \frac{(C_0 - C_t)xv}{M} \qquad 2$$

Where M is the dose (g), V is the volume of the solution (L), and C_t is the concentration of Zn (II) at time t (mg/L). This represents the quantities of Zn (II) adsorbed (mg/g) at time t and equilibrium, respectively, as q_t and q_e.

Pseudo first Order: According to the model, there is a direct proportionality between the variation in the concentration and the rate of adsorbate removal over time and the rate of change in adsorbate uptake at a given reaction time. According to Edet *et al.* (2020), the equation (3) below represents the model, also referred to as the Largergren model:

$$\frac{dq_t}{d_t} = k_t(q_e - q_t) \qquad 3$$

Where k_t is the pseudo-first-order adsorption rate constant (min^{-1}) and q_e and q_t are the adsorbent's adsorption capacities at equilibrium and time, respectively, in mg/g. Equation 3 integral form

becomes once boundary conditions are applied, t = 0 to t = t and q_t = 0 to q_t = q_e.:

$$Log(q_e - q_t) = (q_e) - \frac{k_1}{2 \cdot 303}t \qquad 4.$$

Upon a linear correlation between t and the values of log ($q_e - q_t$). Log ($q_e - q_t$) vs t provides a linear connection from which k_t and q_e may be extracted from the plot's slope and intercept.

Pseudo Second Order: As per Ademiluyi and Nze (2016), the pseudo-second-order adsorption kinetics rate equation may be written as follows:

$$\frac{dq_t}{d_t} = k_2(q_e - q_t)^2 \qquad 5$$

Where k_2 (g/mg/min) is the pseudo-second-order adsorption rate constant.

The equation with the boundary conditions t=0 to t=t and qt=0 to q_t=q_e takes on the following integral form:

$$\frac{1}{q_e - q_t} = \frac{1}{q_e} + k_t \qquad 6$$

Langmuir-isotherm: Adsorption on a homogenous surface is studied using this isotherm. The adsorption processes that follow this isotherm include no contact between the adsorbed molecules. Adsorption is thought to occur in a single layer, with a uniform distribution of adsorption energy on the adsorbent surface, with the majority of adsorption being dependent on the saturation level of that single adsorption layer (Alyuz and Veli, 2009). Equation (7) presents the linear form of Langmuir isotherm.

$$\frac{C_e}{C_e} = \frac{1}{(q_m b)} + \frac{C_e}{q_m} \qquad 7$$

Where b is the Langmuir constant (L/mg), q_e is the quantity of contaminant absorbed per gramme of the adsorbent (mg/g), and Ce is the contaminant concentration at equilibrium (mg/L) (Langmuir, 1916). Plotting values of $\frac{1}{q_e}$ versus $\frac{1}{C_e}$ allowed for the creation of the diagram and the extraction of the linear equation.

Freundlich Isotherm: Adsorption occurs on a heterogeneous surface of a multilayer adsorbent and interactions occur between adsorbent molecules during the adsorption process if the adsorption isotherm follows the Freundlich isotherm. Additionally, this isotherm demonstrates that during the adsorption process, the adsorption energy of the adsorbing centres decreases (Mansourian *et al.*, 2016).

Equation (8) presents the linear form of the Freundlich isotherm, as explained by Darvishmotevalli *et al.* (2019).

$$\ln q_e = \ln K_f + \left(\frac{1}{n}\right)\ln C_e \qquad 8$$

Where C_e is the contaminant concentration at equilibrium; K_f is the Freundlich constant and a relative measure of adsorption capacity (mg/g); and n denotes adsorption intensity. q_e is the quantity of the contaminant adsorbed per gramme of the adsorbent (mg/g) under equilibrium circumstances.

A high value for n indicates that the adsorption procedure is desirable (Matej *et al.*, 2021). The linear equation for this isotherm was found by plotting the values of $\ln(q_e)$ against those of $\ln(C_e)$. Values of n larger than 1 indicate a favourable physical adsorption process (Stylianos *et al.*, 2020). The adsorption's heterogeneity factor is represented by $\frac{1}{n}$. Adsorption is heterogeneous if the value of this component falls between 0 and 1, homogeneous if it is less than zero, and a mix of homogeneous and heterogeneous circumstances if it is larger than 1 (Kumar *et al.*, 2010; Absalan *et al.*, 2011).

RESULTS AND DISCUSSION

Effect of Initial Zinc Concentration: The impact of the initial zinc concentration on the effectiveness of adsorption is shown in Fig. 1. There is a decrease in removal efficiency using doses that range from 10 to 100 mg/L. This pattern suggests that at lower concentrations, there are sufficient adsorption sites available for zinc ions. However, as the concentration of zinc increases, the adsorption sites of the DES nanoparticles become saturated, leading to a decrease in removal efficiency. After the saturation point, removal efficiency decreases because the analytes need more energy to overcome the boundary layer effect (Garg and Gupta, 2004).
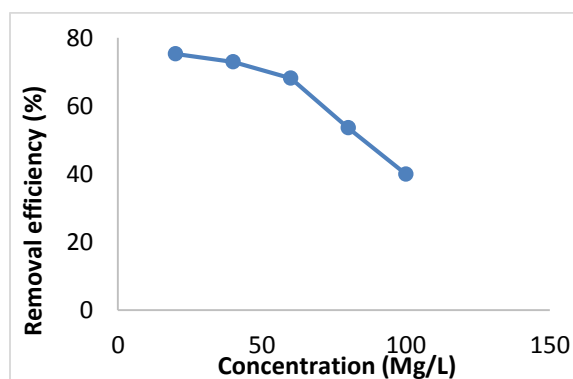

Fig.1: Effect of concentration on adsorption of Zn (II) ion onto Deep eutectic solvent (DES)

Effect of Contact Time: According to Absalan *et al.* (2011), contact time is a crucial optimisation parameter that determines the maximum amount of time an analyte may be removed from an aqueous medium by adsorption. Fig. 2 illustrates how contact time affects zinc adsorption. After a sharp increase in the first 30 minutes, the adsorption efficiency grew more slowly until equilibrium was attained after around sixty minutes. This typically occurs in adsorption processes, because initially there are many accessible adsorption sites, leading to rapid absorption. Because the material surface and analyte repel one another, it gets harder to fill the remaining vacant spots as the contact duration increases (Gopal *et al.,* 2019).
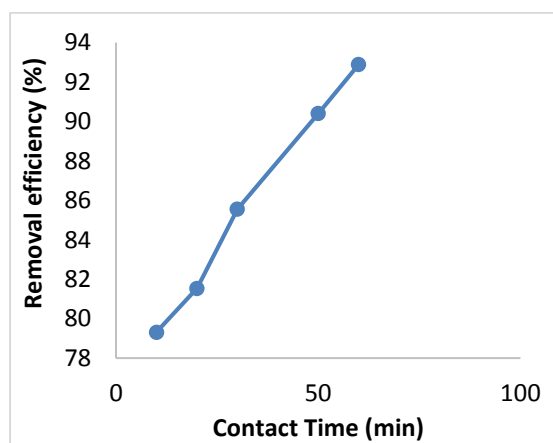

Fig.2: Effect of contact time on adsorption of Zn (II) ion onto Deep eutectic solvent (DES)

Effect of Temperature: Analysing the stability and binding ability of the DES nanomaterial involved examining the impact of temperature. For each analyte, the temperature was raised from 10 °C to 20, 30, 40, 50, 60, and 70 °C. As shown in Fig. 3, the efficiency of the adsorption process declined with increasing temperature and peaked at lower temperatures. This implies that the adsorption process is exothermic, or driven by a decrease in free energy, which explains why an increase in temperature damages the advantageous interactions between the adsorbent (DES nanoparticles) and the adsorbate zinc (II) ion, resulting in a decrease in adsorption efficiency.

Effect of pH: Fig. 4 depicts the effect of pH on zinc adsorption. According to Silva *et al.* (1996), pH has the potential to alter the dissociation of functional groups on the adsorbent's active sites, the adsorbent's surface charge, and the current state of the adsorbate molecule. An increase in removal efficiency at pH 7 compared to lower efficiencies recorded at both acidic and alkaline pH levels indicates an optimal pH condition for DES nanoparticles Zn (II) ion adsorption. Low pH causes protons to compete with zinc ions for

adsorption sites, lowering efficiency. At high pH, zinc may form hydroxide complexes, which are less likely to be adsorbed. This suggests that at pH 7, the surface charge or other chemical properties of the nanoparticles enhance the affinity for Zn (II), leading to higher removal efficiency.
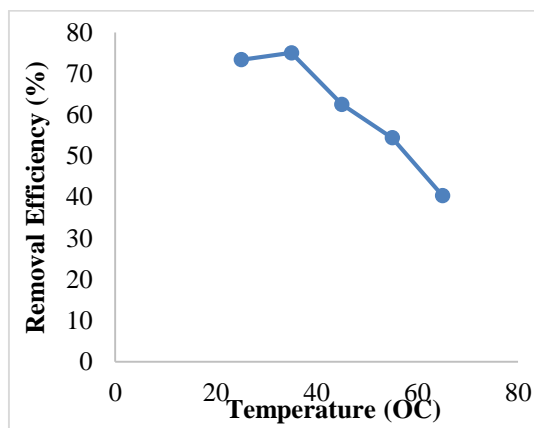

Fig.3: Effect of temperature on adsorption of Zn (II) ion onto Deep eutectic solvent (DES)
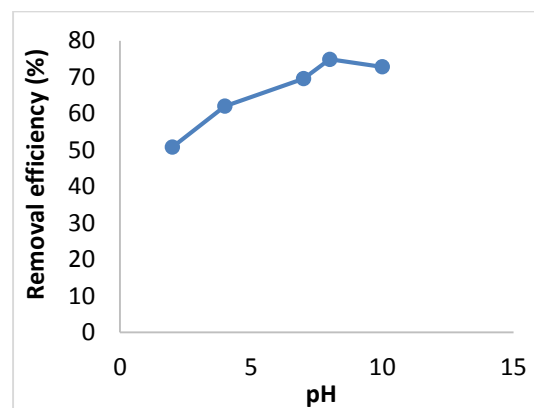

Fig.4: Effect of pH on adsorption of Zn (II) ion onto Deep eutectic solvent (DES)

Effect of Adsorbent Dosage: Fig. 5 illustrates that the DES nanoparticles exhibited a dosage-dependent behavior in removing the Zn (II) ion, increasing the adsorbent dosage led to an increase in removal efficiency. This is because there are more active sites available or adsorption capacity as the dosage of the nanoparticle is added (Matej *et al*., 2021). However, the rate of increase in efficiency slows at higher dosages, demonstrating the existence of an ideal dose at which any increases could not be financially feasible. The collection of adsorbent made it harder for the analytes to react with the binding sites, even though there were many more active sites accessible due to the rise in adsorbent quantity (Gopal *et al.,* 2019), which overlapped. This resulted in no obvious variation in the removal percentage even after

increasing the dosage amount. Hence, 10 mg was selected as the equilibrium dosage for the analytes.
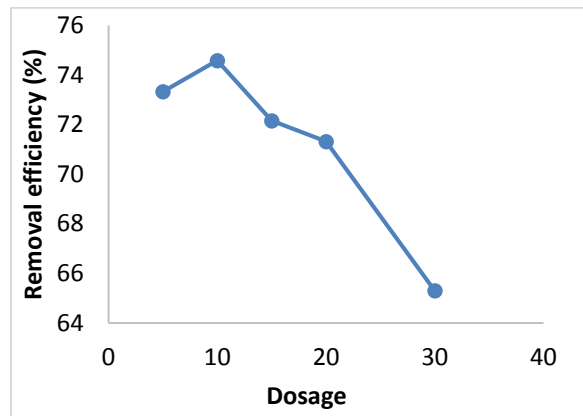

Fig.5: Effect of dosage on adsorption of Zn (II) ion onto Deep eutectic solvent (DES)

Adsorption Kinetics: As shown in Table 1, the pseudo-second-order model's R^2 value of 0.9130 is nearer to one (1) than the pseudo-first-order model's value of 0.4013. This suggests that in comparison to the pseudo-first-order model, the pseudo-second-order model had a higher correlation, provided a better fit for the experimental data, and more accurately represented the system's adsorption kinetics.

Table 1: Kinetic parameters for the adsorption of Zn (II) ion

Kinetic model	Parameters	Material (DES, Fe_3O_4)	Literature values
Pseudo first order	q_e exp (mg/g)	7.488	16.31
	q_e cal (mg/g)	5.546	1.830
	K min^{-1}	0.0559	0.015
	R^2	0.4013	0.670
	RE (%)	25.934%	-
Pseudo second order	q_e cal (mg/g)	6.8212	15.77
	K_2 (g/mg/min)	0.0160	0.094
	h(mg/g/min)	0.7449	-
	R^2	0.9186	0.999
	$t_{1/2}$ (min)	0.0023	-
	RE (%)	8.904	-

According to pseudo-second-order kinetics in adsorption processes, The Square of the adsorbate concentration on the adsorbent surface directly determines the rate of adsorption (Stylianos *et al.,* 2020). According to these findings, the rate-determining step in the adsorption process is the chemisorption of the adsorbate onto the adsorbent surface. This result is also similar to the one obtained by (Matej *et al*., 2021).

Figures 6 and 7 illustrate the Freundlich and Langmuir model of the process. The R^2 value for the Langmuir model (0.9740) is closer to one (1) than the R^2 value for the Freundlich model (0.7660), suggesting that the

Langmuir model is a more appropriate representation of the adsorption process. These indicate that the DES materials have a monolayer adsorption on a homogeneous surface. The maximum adsorption capacity (q_m) was 22.883 mg/g as shown in Table 2.
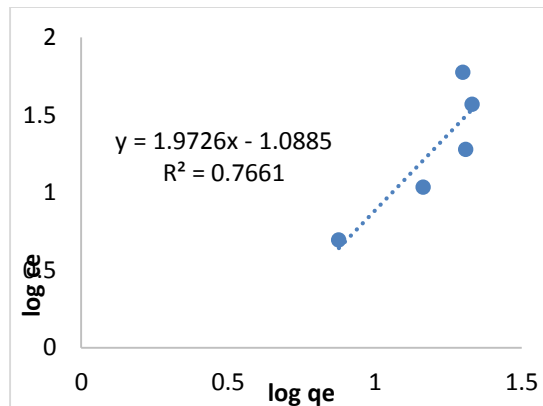

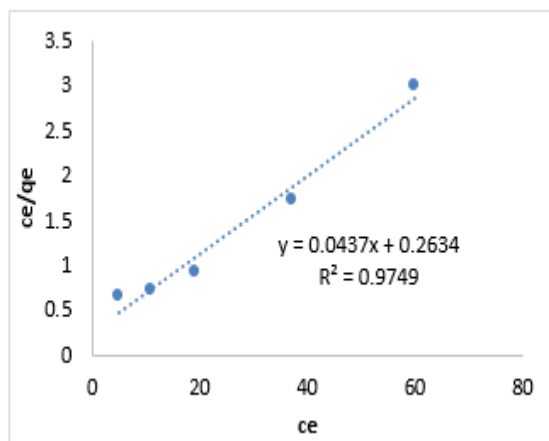**Fig.6:** Freundlich isotherm model for Zn (II) ion adsorption

Fig.7: Langmuir isotherm model for Zn (II) ion adsorption

Table 2: Isotherm parameters for the adsorption of Zn (II) ion

Isotherm model	Parameters	Temp. (25°C)	Literature Value (Matej *et al.,* 2021.)
Langmuir	q_m exp (mg/g)	22.883	27.79
	b (L/mg)	0.1659	0.417
	R^2	0.9740	0.999
	RL	0.0912	0.056
Freundlich	K_F [(mg/g) (L/mg)1/n]	12.2602	10.170
	n	0.5793	-
	1/n	1.7260	0.173
	R^2	0.7661	0.999

The result consistently supports the finding in Fig 1 that efficiency decreases as concentration increases. It also shows that DES has varying affinities for the Zn (II) ion adsorbate and the adsorption process is best at lower concentrations, this invariably confirms the result in Fig. 1 where there is a decrease in efficiency when the concentration increases. This is also in

agreement with the result obtained by Matej *et al.* (2021).

Conclusion: Zinc (II) ions can be effectively removed from aqueous solutions using DES nanoparticles, as demonstrated by this work. High Zn (II) ion removal efficiency is demonstrated by DES at ambient temperature and neutral pH. With pseudo-second-order kinetics and the Langmuir isotherm model, the adsorption process is most accurately approximated, suggesting a chemisorption process on a homogeneous surface. This therefore shows that DES nanoparticles have an enormous potential as an environmentally friendly and efficient adsorbent for zinc removal from water, contributing to the development of sustainable water treatment systems.

Declaration of Conflict of Interest: The authors declare no conflict of interest.

Data Availability Statement: Data are available upon request from the corresponding author.

REFERENCES:

Absalan, G; Asadi, M; Kamran, S; Sheikhian, L; Goltz, DM (2011). Removal of reactive red-120 and 4-(2-pyridylazo) resorcinol from aqueous samples by Fe_3O_4 magnetic nanoparticles using ionic liquid as a modifier. *J. Hazard. Mater.* 192: 476–484. DOI: https://doi.org/10.1016/j.jhazmat.2011.05.046.

Ademiluyi, FT; Nze, JC (2016). Sorption characteristics for multiple adsorptions of heavy metal ions using activated carbon from Nigerian bamboo. *J. Mat. Sci. Chem Eng*. 4:39-48. DOI: 10.4236/msce.2016.44005

Alyüz, B; Veli, S (2009). Kinetics and equilibrium studies for the removal of nickel and zinc from aqueous solutions by ion exchange resins. *J. Hazard. Mater.* 167(1–3): 482–488. DOI: 10.1016/j.jhazmat.2009.01.006

Artioli, Y (2017). Adsorption: Encyclopedia of Ecology. Academia press. Pages 60-65.

Bose, P; Deb, D; Bhattacharya, S (2018). Ionic liquid-based nanofluid electrolytes with higher lithium salt concentration for high-efficiency, safer, lithium metal batteries. *J. Power Sources.* 406: 176–184. DOI: https://doi.org/10.1016/j.jpowsour.2018.10.050

Darvishmotevalli, M; Salari, M; Moradnia, M; Heydari, M; Kiani, G; Fadaei, S; Karimi, H; Bina, B (2019). Evaluation of magnetic ZSM-5 composite performance in 2, 4 dichlorophenol removal from synthetic solutions: response surface method (RSM) modeling and isotherm, kinetic and thermodynamic studies. *Desal. Water Treatment*. 164: 249–262. DOI: 10.5004/dwt.2019.24451

Deroche, L; Devaux, S (2019). Etude bibliographique sur. École des Mines de Douai, Douai, France, Pp. 1-42.

Edet, UA; Ifelebuegu, AO (2020). Kinetics, isotherms, and thermodynamic modeling of the adsorption of phosphates from model wastewater using recycled brick waste. *Processes*. 8(665): 1-15. DOI: https://iopscience.iop.org/article/10.1088/1

Garg, VK; Gupta, KR (2004). Removal of malachite green dye from aqueous solution by adsorption using agro-industry waste: a case study of Prosopis cineraria. *Dyes Pigm*. 62(1): 1-10. DOI:10.1016/j.dyepig.2003.10.016

Gopal, K; Mohd, NI; Raoov, M; Suah, FBM; Yahaya, N; Zain, NNM (2019). Development of a new efficient and economical magnetic sorbent silicone surfactant-based activated carbon for the removal of chloro- and nitro-group phenolic compounds from contaminated water samples. *RSC Adv*. 9: 36915. DOI: 10.1039/c9ra0715

Kumar, PS; Ramalingam, S; Senthamarai, C; Niranjanaa, M; Vijayalakshmi, P; Sivanesan, S (2010). Adsorption of dye from aqueous solution by cashew nut shell: Studies on equilibrium isotherm, kinetics and thermodynamics of interactions. *Desalination*. 261: 52–60. DOI: https://doi.org/10.1016/j.desal.2010.05.032

Langmuir, I (1916). The constitution and fundamental properties of solids and liquids. Anal. Chem. Soc. 38: 2221–2295. DOI: http://dx.doi.org/10.1021/ja02268a002

Larakeb, M; Youcef, L; Achour, S (2016). Removal of Zinc from water by adsorption on different adsorbents. *J. New Techno. Mat.* 6(1):19-25. DOI: http://doi.org/10.12816/0043919

Mansourian, N; Javedan, G; Darvishmotevalli, M; Sharafi, K; Ghaffari, HR; Sharafi, H; Arfaeinia, H; Moradi, M (2016). Efficiency evaluation of zeolite powder, as an adsorbent for the removal of nickel and chromium from aqueous solution: Isotherm and kinetic study. *Int. J. Pharm. Techno*l. 8(2): 13891–13907.

Matej, A; Dusek, M; Zelezny, V; Vrana, J; Sedmidubsky, D (2021). Experimental and theoretical investigation of deep eutectic solvents based on choline chloride. *J. Mol. Liq.* 337: 116452. DOI: http://doi.org/10.1016/j.molliq.2021.116452

Sawyer, AN; McCarty, PL; Parkin, GF (2018). Chemistry for Environmental, Engineering, and Science: 5th ed. Mc-Graw Hill. Pp. 1-741.

Silva, F; Ume, JI; Scamni, AW; Radovic, LR (1996). Effects of surface chemistry of activated carbon on the adsorption of aromatics containing electron withdrawing and electron donating functional groups. *ACS Divi. Fuel Chem., Preprints.* 41(1): 461-463.

Singh, A; Sharma, AK; Verma, RL; Chopade, RP; Pandit, P; Nagar, VS; Sankhla, M. (2022). Heavy metal contamination of water and their toxic effect on living organisms. *IntechOpen*. DOI: 10.5772/intechopen.105075

Stylianos S, N; Karl, P; Andrew, SR; Koen, PA; Koen B; Sofia R (2020). Separation of iron (III), zinc(II), and lead(II) from a choline chloride–ethylene glycol deep eutectic solvent by solvent extraction. *RSC Adv*. 10: 33161-3317. DOI: http://doi.org/10.1039/d0ra06091g

Ümit, YY; Rüstem, K; Chaudhery, MH (2024). Green and sustainable chemistry, Pages 3-25, ISBN 9780443154317. DOI: https://doi.org/10.1016/B978-0-443-15431-7.00014-3

Veli, S; Alyuz, B (2007). Adsorption of Copper and Zinc from Aqueous Solutions by Using Natural Clay. J. Hazard. Mat. 149: 226–233. DOI: https://doi.org/10.1016/j.jhazmat.2007.04.109

Walvekar, R; Chen, YY; Saputra, R; Khalid, M; Panchal, H; Chandran, D; Muabrak, NM; Sadasivuni, KK (2021). Deep eutectic solvents-based CNT nanofluid – A potential alternative to conventional heat transfer fluids. J. Taiwan Inst. Chem. Eng. 128: 314–326. DOI: https://doi.org/10.1016/j.jtice.2021.06.017

WHO (2022). Guidelines for Drinking-water Quality: 4th edition incorporating the 1st and 2nd addenda. World Health Organization Geneva.